arXiv:1404.3554v1 [nucl-th] 14 Apr 2014

The relativistic Green's function model in charged-current quasielastic neutrino and antineutrino scattering at MINERνA kinematics

Andrea Meucci and Carlotta Giusti
Dipartimento di Fisica, Università degli Studi di Pavia and INFN, Sezione di Pavia, via A. Bassi 6, I-27100 Pavia, Italy

(Dated: April 15, 2014)

The analysis of charged-current quasielastic neutrino and antineutrino-nucleus scattering cross sections requires relativistic theoretical descriptions also accounting for the role of final-state interactions. We compare the results of the relativistic Green's function model with the data recently published by the MINERνA Collaboration. The model is able to describe both MINERνA and MiniBooNE data.

PACS numbers: 25.30.Pt; 13.15.+g; 24.10.Jv
Keywords: Neutrino scattering; Neutrino-induced reactions; Relativistic models

I. INTRODUCTION

In the past decade several Collaborations have presented their results of neutrino oscillations [1–19] that aim at a precise determination of mass-squared splitting and mixing angles in ν_μ disappearance and ν_e appearance measurements. In addition, various experimental neutrino-nucleus differential cross sections have been published [20–27] and other measurements are planned in the near future. The reduction of uncertainties in baseline neutrino oscillation experiments is mandatory to obtain a deeper understanding of neutrino physics. In this spirit, since experiments are performed with detectors made of heavy nuclear targets, e.g, Carbon, Oxygen, or Argon, a clear understanding of nuclear effects is extremely important for the analysis of data. The recent progress, the questions and challenges in the physics of neutrino cross sections are reviewed in [28, 29].

The MINERνA Collaboration has recently measured differential cross sections for neutrino and antineutrino charged-current quasielastic (CCQE) scattering on a hydrocarbon target in an energy range between 1.5 and 10 GeV [30, 31]. A large fraction of the total reaction cross section at the GeV energy scale can be ascribed to CCQE reactions, defined in this case as containing no mesons in the final state, that can therefore be viewed as a reference for neutrino oscillation experiments in this energy range.

The first measurements of the CCQE flux-averaged double-differential $\nu_\mu(\bar{\nu_\mu})$ cross section on ^{12}C in the few GeV region by the MiniBooNE Collaboration [20, 22] have raised extensive discussions. Indeed, the fact that the experimental cross sections are usually underestimated by the relativistic Fermi gas model and by other more sophisticated models based on the impulse approximation (IA) [32–36], unless the nucleon axial mass is significantly enlarged, up to $M_A \sim 1.2 \div 1.4$ GeV/c^2, with respect to the world average value of 1.03 GeV/c^2 [37, 38], have suggested that effects beyond the IA may play a significant role in this energy domain [39–48].

Models developed for QE electron scattering [49, 50] and able to successfully describe a wide number of experimental data can provide a useful tool to study neutrino-induced processes. In particular, a reliable description of the effects of the final-state interactions (FSI) between the ejected nucleon and the residual nucleus is very important for the comparison with data. The important role of FSI has been clearly stated for the exclusive $(e, e'p)$ reaction within the framework of the distorted-wave impulse approximation (DWIA), where the use of a complex optical potential (OP) with its absorptive imaginary part produces a reduction of the calculated cross section that is essential to reproduce the data. The imaginary part of the OP accounts for the fact that in the elastic nucleon-nucleus scattering, if other channels are open besides the elastic one, part of the incident flux is lost in the elastically scattered beam and goes to the inelastic channels which are open. In the exclusive $(e, e'p)$ reaction only one channel contributes and it is correct to account for the flux lost in the selected channel. In the case of the inclusive (e, e') reaction, as well as of CCQE neutrino scattering, all elastic and inelastic channels contribute, the total flux is redistributed in all the channels but must be conserved, and the use of the DWIA with an absorptive complex OP is conceptually wrong. Different approaches have been adopted within the framework of the relativistic IA (RIA) to describe FSI in the inclusive QE electron and neutrino-nucleus scattering.

In the relativistic plane-wave impulse approximation (RPWIA) FSI are neglected. The results of this simple approach are usually significantly different from the data and, in addition, they do not reproduce the behavior of the phenomenological

scaling function extracted from QE longitudinal (e, e') data [51, 52]. In other approaches based on the RIA, FSI are included in the emitted nucleon state with real potentials, either retaining only the real part of the relativistic energy-dependent complex optical potential (rROP), or using distorted waves obtained with the same relativistic energy-independent potentials considered in describing the initial nucleon state (RMF) [51, 53, 54].

In the relativistic Green's function (RGF) model FSI are described in the inclusive scattering consistently with the exclusive scattering by the same complex OP, the components of the nuclear response are written in terms of matrix elements of the same type as the DWIA ones of the exclusive $(e, e'p)$ process, but involve eigenfunctions of the OP and of its Hermitian conjugate, where the opposite sign of the imaginary part gives in one case an absorption and in the other case a gain of strength. The imaginary part is therefore responsible for the redistribution of the flux in all the channels and in the sum over all the channels the total flux is conserved. The RGF model has been extensively tested against QE (e, e') data over a wide energy range and for different target nuclei [55–58]. The detailed description of the model can be found in our previous papers [55, 56, 59–64].

Thes results of these different descriptions of FSI have been compared in [56] for the inclusive QE electron scattering, in [63] for the CCQE neutrino scattering, and in [65, 66] with the CCQE and NCE MiniBooNE data. Electron scattering data and their related scaling functions are successfully described by both RMF and RGF models. In the case of MiniBooNE neutrino data, both models reproduce the shape of the experimental CCQE cross sections, but only the RGF gives cross sections of the same magnitude as the experimental ones without the need to increase the world average value of M_A [64, 65]. The larger RGF cross sections are due to the translation to the inclusive strength of the overall effect of inelastic channels that are recovered in the model by the imaginary part of the relativistic OP and that are not included in the RMF and in other models based on the IA.

It has been pointed out in [67] that IA-based models are able to reproduce the higher energy data from the NOMAD experiment [68]. The kinematics of the MINERνA experiment is higher than MiniBooNE but lower than NOMAD and can be useful to understand the role of nuclear structure, many-body mechanisms, and reaction models in neutrino-nucleus scattering. We note that the RMF model provides a good description of CCQE MINERνA data [54].

In this paper we compare the neutrino and antineutrino CCQE MINERνA cross sections with the results of our RGF model.

II. RESULTS

In all the calculations presented in this work we have adopted the standard value for the nucleon axial mass $M_A = 1.03$ GeV/c^2. The bound nucleon states are taken as self-consistent Dirac-Hartree solutions derived within a relativistic mean field approach using a Lagrangian containing σ, ω, and ρ mesons [69–73]. A crucial ingredient of the RGF calculations is the relativistic OP. We have used two different parametrizations for the OP of ^{12}C: the Energy-Dependent and A-Independent EDAI (where the E represents the energy and the A the atomic number) OP of [74], and the more recent Democratic (DEM) phenomenological OP of [75]. The EDAI OP is a single-nucleus parametrization which is constructed to better reproduce the elastic proton-^{12}C phenomenology, whereas the DEM parametrization is a global parametrization, which depends on the atomic number A and is obtained through a fit to more than 200 data sets of elastic proton-nucleus scattering data on a wide range of nuclei that is not limited to doubly closed shell nuclei. In comparison with electron scattering data, the DEM parametrization produces in general good results for doubly magic nuclei and less good but still acceptable results for nuclei with a number of nucleons far from the magic numbers [57, 58].

In Figs. 1 and 2 we present the differen-

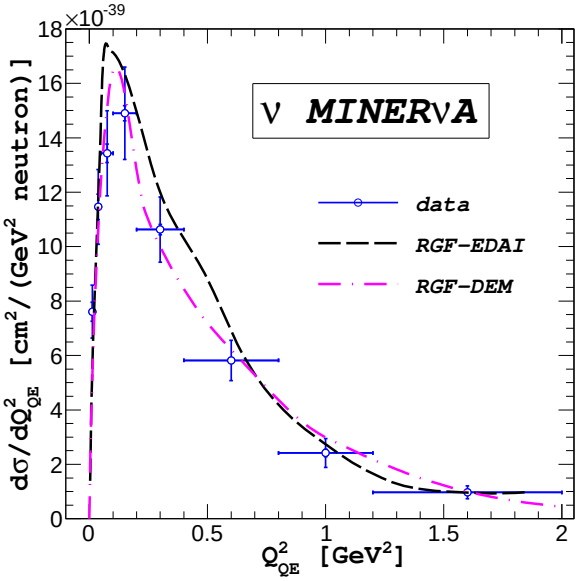

Figure 1. (Color online) CCQE flux-averaged $\nu-^{12}$C cross section per target nucleon as a function of Q^2_{QE}. The data, with statistic and systematic errors, are from MINERνA [30].

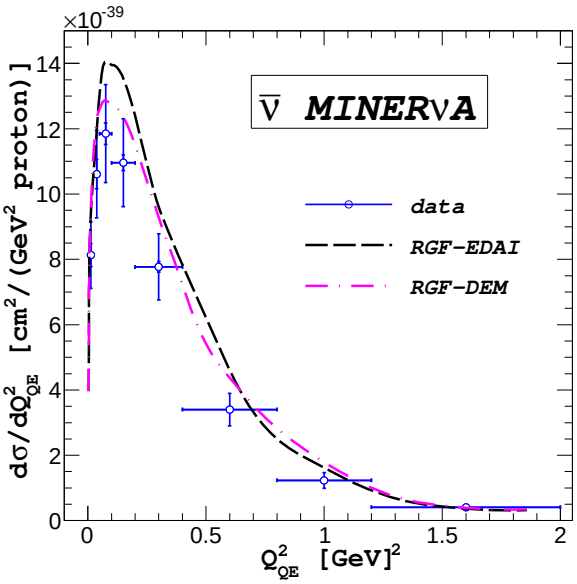

Figure 2. (Color online) CCQE flux-averaged $\bar{\nu}-^{12}$C cross section per target nucleon as a function of Q^2_{QE}. The data, with statistic and systematic errors, are from MINERνA [31].

tial cross section $d\sigma/dQ^2_{QE}$ for neutrino and antineutrino scattering off a CH target as a function of the reconstructed four-momentum transfer squared Q^2_{QE}, which is obtained, as for the experiment, assuming an initial state nucleon at rest with a constant binding energy set to 34 MeV (30 MeV) in the neutrino (antineutrino) case. The calculated cross sections are then folded with the MINERνA neutrino and antineutrino fluxes and compared with the experimental data of [30, 31].

The RGF cross sections in Figs. 1 and 2 are in good agreement with the data. Both RGF-EDAI and RGF-DEM results are within the error bars in the entire kinematical range of MINERνA. The RGF-EDAI cross sections are, however, larger than the RGF-DEM ones in the low four-momentum transfer squared region, $Q^2_{QE} \lesssim 0.5$ GeV^2, while similar results are obtained with the two OPs for larger values of Q^2_{QE}. The differences between the two RGF results are due to the different imaginary parts of the relativistic OPs adopted in the calculations, that can give large differences in the neutrino-nucleus cross sections at different energy and momentum transfer. We note, however, that the differences are generally small and, in the case of antineutrino cross sections in Fig. 2, they are always less than 10%.

A larger sensitivity to the choice of the relativistic OP is obtained at the MiniBooNE kinematics. The results can be found in [64, 65], where it is also shown that the RGF calculations are, in general, in satisfactory agreement with the MiniBooNE cross sections.

An example of the comparison with the Mini-

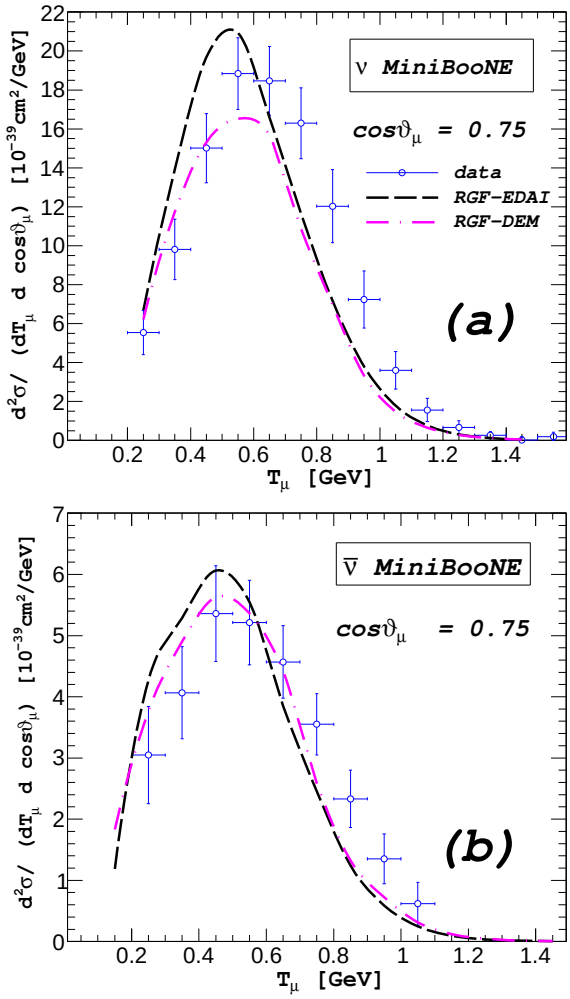

Figure 3. (color online) Flux-averaged double-differential cross section per target nucleon for the CCQE neutrino [panel (a)] and antineutrino [panel (b)] reaction as a function of outgoing muon kinetic energy T_μ for the $\cos\vartheta_\mu = 0.75$ angular bin. The data are from MiniBooNE [20, 22].

BooNE data is presented in Fig. 3, where the RGF CCQE double-differential neutrino (antineutrino) cross sections averaged over the MiniBooNE fluxes are displayed as a function of the muon kinetic energy T_μ for the $\cos\vartheta_\mu = 0.75$ angular bin. The RGF-EDAI results have been already published in [64, 65] and are shown here for completeness. The RGF-DEM cross sections are only a bit larger but in general close to the results obtained in [64, 65] with the EDAD1 optical potential, which corresponds to a less recent energy-dependent and A-dependent parametrization [74]. Both RGF results in Fig. 3 are in reasonable agreement with the data around the peak region, while the data are slightly underpredicted for large T_μ. In contrast, other models based on the IA underestimate the MiniBooNE cross sections and suggest that non-

QE processes induced by two-body currents can play an important role at MiniBooNE kinematics. Our results in Figs. 1, 2, and 3 show the same qualitative behavior and in general a satisfactory agreement in comparison with both MiniBooNE and MINERνA data.

The very recent analysis in [54], which makes use of the SuperScaling Approximation (SuSA) [76] and of the RMF approach to neutrino scattering, shows that these two models, which both underestimate the MiniBooNE data if the value $M_A = 1.03$ GeV/c^2 is adopted in the calculations, provide, with the same value of M_A, a good description of the MINERνA data. This is an indication that there is no need to enlarge the axial mass or to invoke any significant contribution from 2p-2h meson exchange currents and other effects beyond the IA to reproduce the MINERνA data. Our RGF cross sections at MiniBooNE kinematics in [64, 65] are significantly larger than the RMF and SuSA ones and in better agreement with the MiniBooNE CCQE data. The differences between our RGF and the RMF and SuSA results are reduced at MINERνA kinematics. This is an indication that in this kinematic situation the relevance of the inelastic contributions included in the RGF is reduced. The RGF cross sections Figs. 1 and 2 are, however, still somewhat larger than the RMF and SuSA ones of [54] but in agreement with the data within the experimental errors.

In Table I we report the values of the total neutrino and antineutrino cross sections per nucleon flux-averaged over the experimental fluxes from 1.5 to 10 GeV. The results corresponding to the two RGF calculations well reproduce the experimental result in the case of neutrino scattering. In the case of antineutrino scattering, the RGF results are a bit larger than the measured cross section but in agreement with the experimental value within one standard deviation in the case of RGF-DEM and within two standard deviations in the case of RGF-EDAI. The SuSA and RMF results of [54] are also shown for a comparison: they are smaller than the RGF results and in good agreement with the data.

Table I. Results for the flux integrated total neutrino and antineutrino CCQE cross section per nucleon compared with the data from MINERνA [30, 31].

Neutrino	σ [10^{-38}cm^2/neutron]
RGF-EDAI	0.97
RGF-DEM	0.91
RMF [54]	0.901
SuSA [54]	0.828
Experimental [30]	0.93 ± 0.01 (stat) ± 0.11 (syst)
Antineutrino	**σ [10^{-38}cm^2/proton]**
RGF-EDAI	0.71
RGF-DEM	0.68
RMF [54]	0.583
SuSA [54]	0.550
Experimental [31]	0.604 ± 0.008 (stat) ± 0.075 (syst)

III. CONCLUSIONS

In this paper we have compared the predictions of the RGF model with the CCQE neutrino and antineutrino-nucleus scattering MINERνA data. The RGF model is able to give a satisfactory description of electron scattering cross sections in the QE region and also of the CCQE MiniBooNE data without the need to increase the standard value of the axial mass. We have shown that the RGF results obtained with the standard value of the axial mass are also able to describe MINERνA data for CCQE neutrino and antineutrino scattering.

The RGF results are usually larger than the results of other models based on the IA. The differences depend on kinematics. The RGF model is based on the use of a complex energy-dependent relativistic OP whose imaginary part includes the overall effect of the inelastic channels which give different contributions at different energies. The energy dependence of the OP makes the RGF results sensitive to the kinematic conditions of the calculations. With the use of a phenomenological complex OP the model includes all the allowed final-state channels and not only direct one-nucleon emission processes. The important role of contributions other than direct one-nucleon emission has been confirmed by different independent models in the case of MiniBooNE cross sections [32, 33], but the same conclusion is doubtful in the case of MINERνA data [54].

The RGF model does not include two-body meson exchange currents, but it can include rescattering processes of the nucleon in its way out of the nucleus, non-nucleonic Δ excitations, which may arise during nucleon propagation, with or without real pion production, and also some multinucleon processes. Such contributions are not incorporated explicitely in the model, but can be recovered, to some extent, by the imaginary part of the relativistic OP. The use of a phenomenological OP, however, does not allow us to disentangle and evaluate the role of a specific reaction process. For instance, we cannot disentangle the contribution of some pion emission processes which can be taken into account by the imaginary part of the OP but which have been subtracted in the analyses of CCQE data.

The RGF results are affected by some theoretical uncertainties due to the use of different available parametrizations of the relativistic OP. These uncertainties depend on kinematics and on the specific situation that is considered. A better determination of the OP which fulfills the dispersion relations in the whole energy region of interest is required to reduce the theoretical uncertainties of the model and deserves further investigation.

ACKNOWLEDGMENTS

We thank M. V. Ivanov for useful and helpful discussions in the preparation of the manuscript.

[1] K. Abe *et al.* (Super-Kamiokande Collaboration), Phys. Rev. D **83**, 052010 (2011).
[2] K. Abe *et al.* (Super-Kamiokande Collaboration), Phys. Rev. Lett. **107**, 241801 (2011).
[3] M. Antonello *et al.* (ICARUS Collaboration), Eur. Phys. J. C **73**, 1 (2013).
[4] B. Aharmim *et al.* (SNO Collaboration), Phys. Rev. C **81**, 055504 (2010).
[5] P. Adamson *et al.* (MINOS Collaboration), Phys. Rev. Lett. **107**, 021801 (2011).
[6] P. Adamson *et al.* (MINOS Collaboration), Phys. Rev. Lett. **110**, 251801 (2013).
[7] P. Adamson *et al.* (MINOS Collaboration), (2014), arXiv:1403.0867 [hep-ex].
[8] K. Abe *et al.* (T2K Collaboration), Phys. Rev. D **85**, 031103 (2012).
[9] K. Abe *et al.* (T2K Collaboration), Phys. Rev. Lett. **111**, 211803 (2013).
[10] K. Abe *et al.* (T2K Collaboration), (2014), arXiv:1403.1532 [hep-ex].
[11] A. A. Aguilar-Arevalo *et al.* (MiniBooNE Collaboration), Phys. Rev. Lett. **110**, 161801 (2013).
[12] K. B. M. Mahn *et al.* (MiniBooNE and SciBooNE Collaborations), Phys. Rev. D **85**, 032007 (2012).
[13] G. Cheng *et al.* (MiniBooNE and SciBooNE Collaborations), Phys. Rev. D **86**, 052009 (2012).
[14] Y. Abe *et al.* (Double Chooz Collaboration), Phys. Rev. Lett. **108**, 131801 (2012).
[15] F. P. An *et al.* (Daya Bay Collaboration), Phys. Rev. Lett. **108**, 171803 (2012).
[16] F. P. An *et al.* (Daya Bay Collaboration), Chin. Phys. C **37**, 011001 (2013).
[17] J. K. Ahn *et al.* (RENO Collaboration), Phys. Rev. Lett. **108**, 191802 (2012).
[18] M. H. Ahn *et al.* (K2K Collaboration), Phys. Rev. D **74**, 072003 (2006).
[19] A. Aguilar *et al.* (LSND Collaboration), Phys. Rev. D **64**, 112007 (2001).
[20] A. A. Aguilar-Arevalo *et al.* (MiniBooNE Collaboration), Phys. Rev. D **81**, 092005 (2010).
[21] A. A. Aguilar-Arevalo *et al.* (MiniBooNE Collaboration), Phys. Rev. D **82**, 092005 (2010).
[22] A. A. Aguilar-Arevalo *et al.* (MiniBooNE Collaboration), Phys. Rev. D **88**, 032001 (2013).
[23] Y. Nakajima *et al.* (SciBooNE Collaboration), Phys. Rev. D **83**, 012005 (2011).
[24] C. Anderson *et al.* (ArgoNeuT Collaboration), Phys. Rev. Lett. **108**, 161802 (2012).
[25] A. A. Aguilar-Arevalo *et al.* (MiniBooNE Collaboration), (2013), arXiv:1309.7257 [hep-ex].
[26] K. Abe *et al.* (T2K Collaboration), Phys. Rev. D **87**, 092003 (2013).
[27] K. Abe *et al.* (T2K Collaboration), (2014), arXiv:1403.3140 [hep-ex].
[28] J. G. Morfin, J. Nieves, and J. T. Sobczyk, Adv. High Energy Phys. **2012**, 934597 (2012).
[29] L. Alvarez-Ruso, Y. Hayato, and J. Nieves, (2014), arXiv:1403.2673 [hep-ph].
[30] G. A. Fiorentini *et al.* (MINERvA Collaboration), Phys. Rev. Lett. **111**, 022502 (2013).
[31] L. Fields *et al.* (MINERvA Collaboration), Phys. Rev. Lett. **111**, 022501 (2013).
[32] O. Benhar, P. Coletti, and D. Meloni, Phys. Rev. Lett. **105**, 132301 (2010).
[33] O. Benhar and G. Veneziano, Phys. Lett. B **702**, 433 (2011).
[34] A. V. Butkevich, Phys. Rev. C **82**, 055501 (2010).
[35] A. V. Butkevich and D. Perevalov, Phys. Rev. C **84**, 015501 (2011).
[36] C. Juszczak, J. T. Sobczyk, and J. Zmuda, Phys. Rev. C **82**, 045502 (2010).
[37] V. Bernard, L. Elouadrhiri, and U. G. Meissner, J. Phys. G **28**, R1 (2002).
[38] A. Bodek, S. Avvakumov, R. Bradford, and H. Budd, Eur. Phys. J. C **53**, 349 (2008).
[39] T. Leitner, O. Buss, L. Alvarez-Ruso, and U. Mosel, Phys. Rev. C **79**, 034601 (2009).
[40] T. Leitner and U. Mosel, Phys. Rev. C **81**, 064614 (2010).
[41] A. M. Ankowski and O. Benhar, Phys. Rev. C **83**, 054616 (2011).
[42] E. Fernandez Martinez and D. Meloni, Physics Letters B **697**, 477 (2011).
[43] J. E. Amaro, M. B. Barbaro, J. A. Caballero, and T. W. Donnelly, Phys. Rev. Lett. **108**, 152501 (2012).
[44] J. E. Amaro, M. B. Barbaro, J. A. Caballero, T. W. Donnelly, and J. M. Udías, Phys. Rev. D **84**, 033004 (2011).
[45] M. Martini, M. Ericson, G. Chanfray, and J. Marteau, Phys. Rev. C **81**, 045502 (2010).
[46] M. Martini and M. Ericson, Phys. Rev. C **87**, 065501 (2013).
[47] J. Nieves, I. Ruiz Simo, and M. J. Vicente Vacas, Physics Letters B **721**, 90 (2013).
[48] T. Golan, K. M. Graczyk, C. Juszczak, and J. T. Sobczyk, Phys. Rev. C **88**, 024612 (2013).
[49] S. Boffi, C. Giusti, and F. D. Pacati, Phys. Rept. **226**, 1 (1993).
[50] S. Boffi, C. Giusti, F. D. Pacati, and M. Radici,

Electromagnetic Response of Atomic Nuclei, Oxford Studies in Nuclear Physics, Vol. 20 (Clarendon Press, Oxford, 1996).
[51] C. Maieron, M. C. Martinez, J. A. Caballero, and J. M. Udías, Phys. Rev. C **68**, 048501 (2003).
[52] J. A. Caballero, Phys. Rev. C **74**, 015502 (2006).
[53] J. A. Caballero, J. E. Amaro, M. B. Barbaro, T. W. Donnelly, C. Maieron, and J. M. Udías, Phys. Rev. Lett. **95**, 252502 (2005).
[54] G. D. Megias, M. V. Ivanov, R. González-Jiménez, M. B. Barbaro, J. A. Caballero, T. W. Donnelly, and J. M. Udías, (2014), 1402.1611 [nucl-th].
[55] A. Meucci, F. Capuzzi, C. Giusti, and F. D. Pacati, Phys. Rev. C **67**, 054601 (2003).
[56] A. Meucci, J. A. Caballero, C. Giusti, F. D. Pacati, and J. M. Udías, Phys. Rev. C **80**, 024605 (2009).
[57] A. Meucci, M. Vorabbi, C. Giusti, F. D. Pacati, and P. Finelli, Phys. Rev. C **87**, 054620 (2013).
[58] A. Meucci, M. Vorabbi, C. Giusti, F. D. Pacati, and P. Finelli, Phys. Rev. C **89**, 034604 (2014).
[59] F. Capuzzi, C. Giusti, and F. D. Pacati, Nuclear Physics A **524**, 681 (1991).
[60] A. Meucci, C. Giusti, and F. D. Pacati, Nuclear Physics A **739**, 277 (2004).
[61] F. Capuzzi, C. Giusti, F. D. Pacati, and D. N. Kadrev, Annals of Physics (N.Y.) **317**, 492 (2005).
[62] A. Meucci, C. Giusti, and F. D. Pacati, Nuclear Physics A **756**, 359 (2005).
[63] A. Meucci, J. A. Caballero, C. Giusti, and J. M. Udías, Phys. Rev. C **83**, 064614 (2011).
[64] A. Meucci and C. Giusti, Phys. Rev. D **85**, 093002 (2012).
[65] A. Meucci, M. B. Barbaro, J. A. Caballero, C. Giusti, and J. M. Udías, Phys. Rev. Lett. **107**, 172501 (2011).
[66] R. González-Jiménez, J. A. Caballero, A. Meucci, C. Giusti, M. B. Barbaro, M. V. Ivanov, and J. M. Udías, Phys. Rev. C **88**, 025502 (2013).
[67] G. D. Megias, J. E. Amaro, M. B. Barbaro, J. A. Caballero, and T. W. Donnelly, Physics Letters B **725**, 170 (2013).
[68] V. Lyubushkin *et al.* (NOMAD Collaboration), Eur. Phys. J. C **63**, 355 (2009).
[69] B. D. Serot and J. D. Walecka, Adv. Nucl. Phys. **16**, 1 (1986).
[70] P. G. Reinhard, Rep. Prog. Phys. **52**, 439 (1989).
[71] P. Ring, Prog. Part. Nucl. Phys. **37**, 193 (1996).
[72] G. A. Lalazissis, J. König, and P. Ring, Phys. Rev. C **55**, 540 (1997).
[73] B. D. Serot and J. D. Walecka, Int. J. Mod. Phys. **E6**, 515 (1997).
[74] E. D. Cooper, S. Hama, B. C. Clark, and R. L. Mercer, Phys. Rev. C **47**, 297 (1993).
[75] E. D. Cooper, S. Hama, and B. C. Clark, Phys. Rev. C **80**, 034605 (2009).
[76] J. E. Amaro, M. B. Barbaro, J. A. Caballero, T. W. Donnelly, A. Molinari, and I. Sick, Phys. Rev. C **71**, 015501 (2005).